Available online at www.sciencedirect.com
SCIENCE DIRECT®
Physica E 17 (2003) 402–405
PHYSICA E
www.elsevier.com/locate/physe

Second-harmonic generation measured on a GaAs photonic crystal planar waveguide

L.C. Andreani[a], F. Cattaneo[a], G. Guizzetti[a], A.M. Malvezzi[a,*], M. Patrini[a], G. Vecchi[a], F. Romanato[b,c], L. Businaro[b,c], E. Di Fabrizio[b,c], A. Passaseo[c], M. De Vittorio[c]

[a] *INFM-Dip. Elettronica and Universitá di Pavia, Via Bassi 6, Via Ferrata 1, I-27100 Pavia, Italy*
[b] *TASC-INFM Trieste, S.S14 Km 163.5, I-34012 Basovizza-Trieste, Italy*
[c] *NNL-INFM, Universitá di Lecce, via per Arnesano, I-73100 Lecce, Italy*

Abstract

Second-harmonic (SH) reflection and diffraction measurements are performed, at the wavelengths of a Ti:sapphire laser on a GaAs/AlGaAs photonic crystal waveguide patterned with a square lattice, the basis consisting of rings of air in the dielectric matrix. The measured angles of diffracted SH beams agree with those predicted from nonlinear diffraction conditions. Results for reflected and diffracted SH intensities as a function of incidence angle, polarization, and pump wavelength show that, due to the low air fraction of the photonic crystal, the reflected one is dominated by the crystalline symmetry of GaAs, while the diffracted one is related to the photonic crystal structure. The large diffraction-to-reflection ratio points to the importance of nonlinear diffraction in photonic crystals. Preliminary measurements in the 1500 nm range reveal explicit features related to photonic modes.

PACS: 42.70.Qs; 81.07.−b

Keywords: Nonlinear optics; Photonic crystals; Second-harmonic generation

1. Introduction

One- and two-dimensional photonic crystal slabs based on GaAs [1] (For recent review see, e.g., [2]) are very well suited for second-harmonic generation (SHG) studies of reflection and diffraction, since the second-order susceptibility of GaAs is large and photonic lattices at optical wavelengths can be defined and patterned deeply on the samples by lithography and etching. In this work we report on SHG measurements in reflection and diffraction from an air/GaAs/$Al_xGa_{1-x}As$ photonic crystal waveguide patterned deeply with a 2D square lattice of air rings. Patterning of the waveguide was performed by X-ray lithography followed by reactive-ion etching (RIE), the mask for X-ray lithography having been generated by electron-beam lithography [3]. The lattice has a low air fraction (about 12%) and an etch depth of more than 1 μm: indeed, linear variable-angle reflectance measurements on this sample [4] showed narrow resonances which point to the existence of low-loss photonic modes, as first shown on triangular lattices of holes in Ref. [5]. The orientation of the

* Corresponding author. Tel.: +39-0382-505512; fax: +39-0382-422583.
E-mail address: malvezzi@ele.unipv.it (A.M. Malvezzi).

1386-9477/03/$ - see front matter
doi:10.1016/S1386-9477(02)00895-0

mask was chosen in such a way that the square axes of the photonic lattices coincide with the crystallographic axis [1 1 0] of GaAs: the [1 0 0] axis of the microscopic lattice (which determines the symmetry properties of the $\chi^{(2)}$ tensor) and the [1 0] axis of the photonic lattice (which produces the diffractive effects) are rotated by 45° with respect to each other.

2. Experimental

The source of excitation for SHG measurements is a Ti:sapphire laser system providing pulses ≈ 130 fs in duration at 80 MHz repetition rate, centered at wavelengths between 750 and 840 nm, with an average power on sample up to 150 mW. The ultrashort pulsed laser is here used to provide sufficiently high intensity for obtaining a detectable SH signal while minimizing thermal load to the sample. Pulses are focused down to 40–50 μm in diameter with a 20 cm focal length lens onto the sample after filtering and control of intensity and polarization. The SH radiation is collected by an optical fiber (400 μm core diameter) and delivered in front of a cooled photomultiplier after passing through a combination of color filters plus a wide-band interference filter which reject the radiation at the pump frequency. No polarization selection of the SH signal has been implemented. The optical fiber is of UV/VIS type, transmitting more than 95% of the radiation at 400 nm.

The geometry of the optical layout is sketched in Fig. 1 where the notations for the angles involved in the experiment are also reported. They are the angle of incidence θ of the pump radiation, the angle ϕ formed by the Γ–X direction of the photonic crystal to the plane of incidence, the polar diffraction angle θ' measured from the normal n to the sample, and the azimuthal angle ϕ' of the diffracted beam measured also from the plane of incidence. Of these four angles, all are variable in the experimental setup except ϕ' which is kept fixed at 0° or 180°. Thus only in-plane diffraction beams (forward and backwards) are being detected while θ' and ϕ are remotely controlled in 0.225 degrees/step increments.

Optical alignment of the setup requires a set of translation stages in order to have the horizontal azimuthal axis of rotation of the sample (defining ϕ) and its vertical axis of rotation (defining θ) to cross at the laser focal spot on the sample surface. Moreover, the rotation of the optical fiber (defining angle θ') has to share the same vertical axis of rotation.

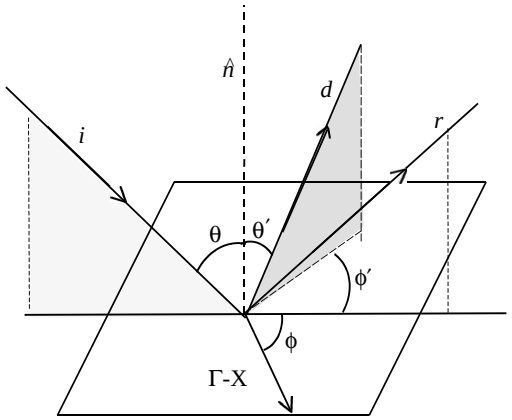

Fig. 1. Geometry of the experiment. The incident (i), reflected (r) and diffracted (d) directions of the beams are indicated, n is the normal to the sample surface and the relevant angles are indicated.

The detection of the SH signal is performed using a light chopper which modulates the pump radiation up to a few kHz. The photomultiplier signal is then recorded by an averaging oscilloscope so that the amplitude of the signal with respect to background is evaluated.

3. Results and discussions

For a given incidence angle and sample orientation, a SH beam is generated in all directions which satisfy the following conditions:

$$\mathbf{k}'_{\parallel} = 2\mathbf{k}_{\parallel} + \mathbf{G}, \tag{1}$$

where $\mathbf{k}_{\parallel}$ ($\mathbf{k}'_{\parallel}$) is the parallel wave vector of the incident (second harmonic) beam and $\mathbf{G}$ is a reciprocal lattice vector of the photonic lattice. For $\mathbf{G} = 0$ we have SHG in reflection. One can view the diffracted SH beam ($\mathbf{G} \neq 0$ in Eq. (1)) as being due to SHG in reflection followed by diffraction at the harmonic frequency, or else diffraction at the pump frequency followed by SHG: the two processes are physically indistinguishable.

The diffraction angles of the SH signal are shown in Fig. 2 versus the angle of incidence θ of the pump beam at 814 nm wavelength. The SH diffracted signals

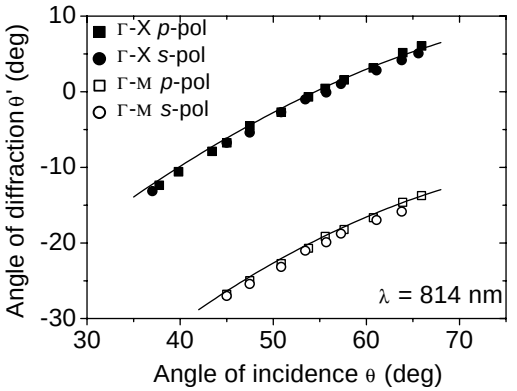

Fig. 2. Measured and calculated angles of diffraction for radiation incident along Γ–X and Γ–M crystal orientations and for s- and p-polarizations, as a function of angle of incidence.

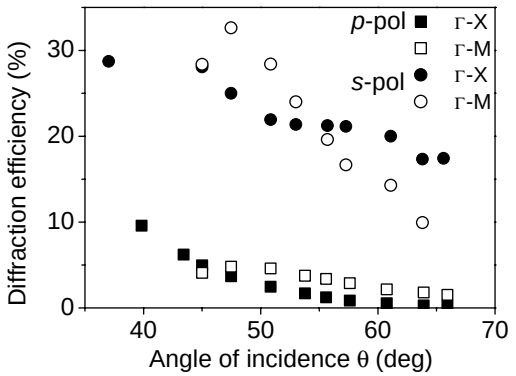

Fig. 3. Diffraction efficiency for the SH radiation generated by 814 nm pump wavelength for the indicated crystal orientations and polarizations.

have been measured both for s- and p-polarization of the incident radiation and both for the Γ–X ($\phi = 0°$) and Γ–M ($\phi = 45°$) photonic crystal orientations. The theoretical SH diffraction curves with $\lambda = 814$ nm are also reported for the two cases. Agreement between the experimental results and the theoretical curves derived from Eq. (1) is very good. The uncertainty over incidence angles is about 1°, due to the alignment procedure both of the sample and of the incident laser beam. In the setup the optical fiber angular position is not absolutely calibrated but is obtained by measuring the position of the SH reflected signal. Thus the uncertainty in the angle of SH reflected and diffracted beams is of the same order as the uncertainty on the incident angle.

For both reflected and diffracted SH measurements, the nonlinear reflection and diffraction coefficients, defined as $R^{NL} = I_R(2\omega)/I(\omega)^2$ and $D^{NL} = I_D(2\omega)/I(\omega)^2$ respectively, have been evaluated [6]. Absolute values for R^{NL} are very similar to those for bulk GaAs and compare favorably with the ones found in the literature [7]. Both photonic crystal orientations give approximately the same R^{NL} value of 8×10^{-23} m^2 W^{-1} for p-polarization and up to 5×10^{-24} m^2 W^{-1} for s-polarization. The small deviation from bulk values seems due to the low air fraction of the sample.

The diffraction efficiency $\eta = D^{NL}/(D^{NL} + R^{NL})$, in the case of s-polarization, is of the order of 30% for both photonic crystal orientations, as shown in Fig. 3, indicating that a consistent fraction of the SH power is diverted by the photonic crystal structure into the diffraction mode. By considering nonlinear diffraction into *all* modes, including those out of the plane of incidence, the value of the diffraction efficiency would be even higher.

The high diffraction efficiency observed is consistent with the trend already observed in the linear case [8] and is a characteristic feature of photonic crystals with large etch depth. These measurements show the key role played by photonic crystal structure in the coupling of incoming electromagnetic radiation generated with a nonlinear crystal such as GaAs. Nonlinear diffraction is uniquely determined by the periodicity of the photonic structure of the sample. On the other hand, the photonic crystal bands of our crystal lie at energies lower than those of the photons used in this experiment. Therefore, no specific features in the SH signals have been observed in this experiment.

In a search for resonant photonic bands signatures, the experiment has been modified by using infrared pulses from an optical parametric oscillator (OPO) in the wavelength interval between 1450 and 1600 nm as a source for excitation. The nonlinear reflectivity of the sample has then been measured as a function of angles of incidence θ and azimuth ϕ for different excitation wavelengths λ. Giant resonances characteristic of nonlinear interaction are observed in the 1.4–1.6 μm range, as shown in Fig. 4 for $\theta = 45°$ and $\lambda = 1540$ nm. These resonance peaks are due to coupling between the incident

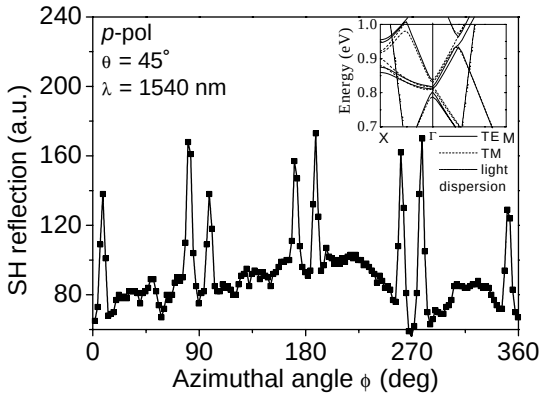

Fig. 4. SH reflection signal from an infrared pump at 1540 nm measured as a function of azimuthal angle for the values of parameters indicated. The inset represents the calculated photonic band diagram in the corresponding energy range.

radiation and the photonic mode at that particular energy and in-plane momentum [9]. The peaks are double and repeated four times in the 360° azimuthal rotation due to the fourfold symmetry of the irreducible inverse cell of the two-dimensional crystal lattice. For comparison with the theory, the calculated photonic bands in the energy region involved are shown in the inset [4].

A preliminary analysis of the results suggests a complete correspondence of the peaks observed in nonlinear reflectivity with those already measured in linear reflectance measurements, the former however being significantly more intense than the latter.

The extreme sensitivity of the nonlinear signal in mapping the band structure of these devices as compared with linear methods in a simple azimuthal reflectance measurement suggests the use of this technique for diagnostic and application purposes.

Acknowledgements

This study was supported in part by INFM PAIS 2001 Project 'DPHOCRY' and by INFM FemtoLab of Pavia. The authors are grateful to Y. Chen and D. Peyrade by LPN-CNRS, Paris, for performing part of the processing of the sample.

References

[1] T.F. Krauss, R.M. De La Rue, S. Brand, Nature 383 (1996) 699.
[2] C.M. Soukoulis (Ed.), Photonic Crystals and Light Localization in the 21st Century, Vol. 563, NATO Science Series C: Mathematical and Physical Sciences, Kluwer, Dordrecht, 2001.
[3] F. Romanato, L. Businaro, E. Di Fabrizio, A. Passaseo, M. De Vittorio, R. Cingolani, M. Patrini, M. Galli, D. Bajoni, L.C. Andreani, F. Giacometti, M. Gentili, D. Peyrade, Y. Chen, Nanotechnology 13 (2002) 644.
[4] M. Galli, M. Agio, L.C. Andreani, L. Atzeni, D. Bajoni, G. Guizzetti, L. Businaro, E. Di Fabrizio, F. Romanato, A. Passaseo, Eur. Phys. J. B 27 (2002) 79.
[5] V.N. Astratov, D.M. Whittaker, I.S. Culshaw, R.M. Stevenson, M.S. Skolnick, T.F. Krauss, R.M. De La Rue, Phys. Rev. B 60 (1999) R16225.
[6] A.M. Malvezzi, F. Cattaneo, G. Vecchi, M. Falasconi, G. Guizzetti, L.C. Andreani, F. Romanato, L. Businaro, E. Di Fabrizio, A. Passaseo, M. De Vittorio, J. Opt. Soc. Am. B 19 (2002) 2122.
[7] R.K. Chang, J. Ducuing, N. Bloembergen, Phys. Rev. Lett. 15 (1965) 415.
[8] D. Labilloy, H. Benisty, C. Weisbuch, T.F. Krauss, R.M. De La Rue, V. Bardinal, R. Houdré, U. Oesterle, D. Cassagne, C. Juanin, Phys. Rev. Lett. 79 (1997) 4147.
[9] A.R. Cowan, J.F. Young, Phys. Rev. B 65 (2002) 085106.